



In situ grafting approach for preparing PLA/PHBV degradable blends with improved mechanical properties

Jiaying Gong¹ · Zhe Qiang² · Jie Ren¹

Received: 7 July 2021 / Revised: 13 October 2021 / Accepted: 28 October 2021 /
Published online: 12 November 2021

© The Author(s), under exclusive licence to Springer-Verlag GmbH Germany, part of Springer Nature 2021

Abstract

A one-step reactive extrusion process has been demonstrated to toughen the poly(lactic acid) (PLA) blend without sacrificing its mechanical strength and degradability. Specifically, poly(lactic acid) (PLA), poly(3-hydroxybutyrate-co-3-hydroxyvalerate) (PHBV), and the peroxide initiator were first introduced into the mixer and then heated at the elevated temperatures for triggering the grafting reaction during the extrusion. During this process, the thermal decomposition of PHBV results in the unsaturated bonds that can directly grafted onto the PLA backbones by free radical reactions. From this study, we found that PLA/PHBV blend with a mass ratio of 80/20 (PLA/PHBV) and 0.3 wt% 2,5-dimethyl-2,5-di(tert-butylperoxy)hexane (DBPH) is an optimized condition, leading to an improved elongation at break of 15.95%, which is 3.1 times of the PLA and 1.5 times of the PLA/PHBV blend without the initiator, while tensile strength exhibited very limited decreased compared to PLA. Overall, this work presents an environmentally friendly and industrial feasible approach to prepare bio-based toughened PLA for improving the elongation at break, while retaining the tensile strength and degradability.

Keywords Poly(lactic acid) · Poly(3-hydroxybutyrate-co-3-hydroxyvalerate) · Reactive blending · Polymer blends · Compatibility

✉ Zhe Qiang
zhe.qiang@usm.edu

✉ Jie Ren
renjie6598@163.com

¹ Institute of Nano and Biopolymeric Materials, Department of Polymeric Materials, Key Laboratory of Advanced Civil Engineering Materials (Ministry of Education), School of Materials Science and Engineering, Tongji University, 4800 Caoan Road, Shanghai 201804, China

² School of Polymer Science and Engineering, University of Southern Mississippi, Hattiesburg, MS 39406, USA

Introduction

Conventional petroleum-derived polymers cause a great burden on the environmental sustainability due to their non-degradable nature [1, 2]. Biodegradable polymers, particularly including poly(lactic acid) (PLA) and poly(3-hydroxybutyrate-co-3-hydroxyvalerate) (PHBV), can provide a feasible solution for the sustainable development of our environment and society [3–7]. Although these polymers are environmentally friendly, their poor mechanical properties make them unsuitable for replacing petroleum-based polymers into the mainstream commodity plastics. PLA is currently the most widely used biodegradable polymer [8–12]. While it has excellent mechanical strength, comparable to some petroleum-based materials, it is also very brittle [13, 14]. PHBV is a recently developed polymer that is produced by bacteria and has very limited mechanical properties, including both elongation at break and tensile strength [15–18]. Research efforts have been concentrated on how to improve the mechanical properties of these environmental-friendly polymers. The common method to improve toughness is through blending with elastomers [19–21], such as using natural rubber, polybutadiene, polyurethane, and poly(ether) urethane, which typically are petroleum-based and non-degradable chemicals/compounds [22–25]. Interestingly, studies have found that while the respective mechanical properties of PLA and PHBV are not excellent, their blends can exhibit much better elongation at break even though the strength is still far from satisfactory due to their chemical incompatibility [26–29].

Reactive extrusion is an effective industrially viable approach to functionalize polymers during processing by covalently attaching unsaturated chemical groups to the backbone of a matrix polymer [30–33]. Among extensive studies on modifying poly(lactic acid) to improve its performance, the commonly used method is through combining reactive extrusion with free-radical-initiated reactions [34–36]. For example, Mo et al. synthesized poly(lactic acid) grafted glycidyl methacrylate (PLA-g-GMA) copolymer and poly(lactic acid) grafted thermoplastic polyurethane (PLA-g-TPU) copolymer, which can be used to improve the compatibility of PLA/TPU blends and enhance the tensile strength [37]. Wang et al. reported a new blend compatibilizer for preparing micro-crystalline cellulose (MCC)/poly(lactic acid) (PLA) composites, which was maleic anhydride-grafted poly(lactic acid) (PLA-g-AMS/MAH) [38]. Due to the addition of PLA-g-AMS/MAH copolymer, mechanical properties of the composites of MCC and PLA were improved significantly. Marsilla et al. grafted itaconic anhydride (IA) to poly(lactic acid) (PLA) and assessed the rate of crystallization of PLA-g-IA [39]. Additionally, blending with fillers is also an alternative method of toughening PLA. Mohamed et al. compounded polylactide (PLA) with organosolv lignin (OL) in the presence of poly(vinyl acetate) and glycidyl methacrylate (GMA). The optimized composites exhibit superior toughness [40]. Most previous studies focused on grafting small molecules containing unsaturated bonds to PLA through reactive extrusion. While these small molecules have good compatibility with polymers, their unreacted residues would migrate to the material surface and

finally be released into the environment to cause adverse impact [41]. Moreover, a random chain scission at ester groups is the mechanism of thermal degradation in PHBV, and the polymer can be thermally degraded to substituted olefins and oligomers [42–44]. The degradation process involves a β -hydrogen elimination process (six-membered ring ester decomposition process), which could enable PHBV to be grafted onto PLA. Compared to other compatibilization methods in blending, in situ grafting between these two polymers is still relatively underexplored [37–39, 45].

In this study, we developed a method to prepare fully bio-based and sustainable materials by a one-step reactive extrusion process, which the addition of the initiator induced the grafting reaction. PHBV produced unsaturated bonds from thermal decomposition, which were then grafted onto the PLA backbone through free radical reactions. Using this approach, we were able to prepare a toughened blend when the mass ratio of PLA and PHBV is 80/20, with the addition of 0.3 wt% 2,5-dimethyl-2,5-di(tert-butylperoxy)hexane. The demonstration of simple and efficient methods for preparing biodegradable polymer blends could be beneficial toward enabling their practical applications.

Experimental section

Materials

Poly(lactic acid) (PLA-6202D) in pellet form was purchased from NatureWorks (USA). The melt index of PLA-6202D is 15–30 g/10 min, and it has a molecular weight of 140 kDa (Mw) with 98% L-lactide to 2% D-lactide units. Poly(3-hydroxybutyrate-co-3-hydroxyvalerate) (PHBV-Y1000P) was purchased from Tianan Biologic Materials Company, Ltd. (China), which has a molecular weight of 280 kDa (Mw) with 8% 3-hydroxyvalerate (3HV) content. The tensile strength of PHBV is 39 MPa, and the elongation at break is approximately 2%. The specific gravity of PLA and PHBV is 1.24 g/cm³ and 1.25 g/cm³, respectively. 2,5-Dimethyl-2,5-di(tert-butylperoxy)hexane (DBPH, Trigonox® 101) was purchased from Aladdin Bio-Chem Technology Company, Ltd. (China) and was used as the initiator for reactive extrusion. Chloroform was obtained from Sinopharm Chemical Reagent Co., Ltd. (China), and d-chloroform was obtained from Meryer Chemical Technology Company, Ltd. (China). All materials were used as received.

Sample preparation

PLA and PHBV were dried under vacuum at 65 °C for 12 h prior to the processing to remove residual water in the sample. This step can reduce the hydrolytic degradation of the polymers during the melt processing. The reactive extrusion was performed by adding all three components (PLA, PHBV, and DBPH) into HAAKE Rheomix QC internal mixer (Thermo Scientific, USA) at 170 °C. The screw speed was set to 40 rpm, and the reaction time was 10 min. Subsequently, blend was removed from

Table 1 Sample name and compositions of different PHBV/PLA blends prepared in this study

Samples	PLA (wt%)	PHBV (wt%)	DBPH (wt%)
100/0	100	–	–
0/100	–	100	–
90/10	90	10	–
80/20	80	20	–
70/30	70	30	–
60/40	60	40	–
80/20D1	80	20	0.1
70/30D1	70	30	0.1
80/20D3	80	20	0.3
70/30D3	70	30	0.3
80/20D5	80	20	0.5
70/30D5	70	30	0.5

the internal mixer and immediately cut it into pellet with scissor while it was hot. A variety of blends with different compositions were prepared, as shown in Table 1. Furthermore, control samples were prepared using PLA and/or PHBV employing the same process. The blended products were collected in the form of pellet, cooled at room temperature, and then dried under vacuum prior to use.

Characterization

The chemical composition of the PHBV/PLA sample before and after heating was determined using ^1H NMR. The AVANCE III HD 400 Nuclear Magnetic Resonance Spectrometer of BRUKER (USA) was used, and the sample was prepared in the *d*-chloroform (CDCl_3) at a concentration of 10 mg/ml. Spotlight 400/400 N (Thermo Scientific Nicolet IS5, USA) was used to recorded the FTIR spectra of various film samples blends. All spectra were recorded in the absorbance mode within wavelength of $4000\text{--}600\text{ cm}^{-1}$. Samples were prepared by solution-casting and dried. The blends were dissolved in chloroform under agitation overnight. The solution was smeared on the glass slide and placed in a fume hood for 12 h. After the solvent evaporated, the film samples were placed in a vacuum oven to be dried at $30\text{ }^\circ\text{C}$ for at least 6 h. The melt flow indices of the blends and the raw materials were determined by MFI452 (WANCE Technologies Company, Ltd., China) under the condition of $190\text{ }^\circ\text{C}/2.16\text{ kg}$, according to the ISO 1133. The MFI of the sample was obtained via Eq. (1):

$$\text{MFI} = \frac{600M}{t} \quad (1)$$

where M is the extrudate weight in grams and t is the time in seconds.

The glass transition, crystallization, and melting temperatures of neat polymers and their blends were obtained by a differential scanning calorimeter (DSC Q 2000, TA Instruments Inc., USA), which was equipped with a cooling attachment, and

the entire operation was under a nitrogen atmosphere. The thermal history of the samples was removed in all measurements. The samples were subjected to a heating ramp from 30 to 200 °C with a rate of 15 °C/min, then cooling to 30 °C at 15 °C/min, and finally a second heating ramp to 200 °C at the same rate. TA Universal Analysis software recorded the heat absorbed and emitted by the sample to the empty aluminum pan as reference for data analysis. The thermal stability of blends was determined by a thermogravimetric analyzer (TGA 2, Mettler Toledo, Switzerland). Sample of approximately 10 mg was loaded into a ceramic cup and scanned from 30 to 600 °C at a heating rate of 10 °C/min under a nitrogen atmosphere.

To investigate the crystallinity of the blends, an X-ray diffractometer (Ultima IV, Rigaku, Japan) was used, and the wavelength of the X-ray beam is 1.5418 nm (using Cu K α -radiation, $V=40$ kV, $I=40$ mA). Measurements were taken over a 2θ range of 5–25°, with a scanning speed of 2°/min.

Tensile testing was used to determine the mechanical properties of the samples. The blends were injection-molded into standard tensile bars according to ISO 20753, using micro-injection molding machine (WZS10D, Shanghai Xinshuo Precision Machinery Co., Ltd.). The cylinder and mold temperatures were 185 °C and 45 °C, respectively. The pressure was 0.4–0.5 MPa, and the holding times were 15 s. At least 5 specimens of each blend composition were prepared for mechanical testing. All samples were pre-conditioned for 24 h before the characterization. Tensile tests were performed on a universal testing instrument (WANCE Technologies Company, Ltd., China). A standard procedure was employed according to ISO 527. Specifically, a crosshead speed of 2 mm/min was used for all dumbbell shaped samples ($75 \times 10 \times 2$ mm³), and data analysis was performed using commercial software.

Hydrolysis tests were performed on blend samples with film geometry. The blended product (0.5 g) was dissolved in chloroform (5 ml) and stirred with a magnet bar for 6 h until a complete homogenous solution was formed. The solutions were slowly poured into glass dishes ($d=4$ cm), evaporated overnight in a fume hood, and then dried in a vacuum oven at 40 °C for 4 h to obtain uniform blend films. The films were placed in 100-ml beakers containing 50 ml phosphate-buffered saline (pH = 7.2–7.4, Adamas life) and hydrolyzed at 80 °C for 2 weeks. Five sets of parallel experiments were performed for each sample. The films were taken out of the aqueous solution, washed with deionized water, dried, and weighed every day. The weight loss (W_{loss}) of the sample was obtained via Eq. (2):

$$W_{\text{loss}} = \frac{m_0 - m_{\text{dry}}}{m_0} \times 100\% \quad (2)$$

where m_0 is the weight (g) prior to hydrolysis and m_{dry} is the weight (g) removed from the hydrolysis media and dried.

The morphology of the blends was determined using a Zeiss Gemini 300 (Carl Zeiss AG, Germany) scanning electron microscope to examine the fracture surface of the samples. Prior to the measurements, specimens were fractured in liquid nitrogen. The specimens were then mounted on a sample stage using conductive glue and coated with a thin gold layer. An accelerating voltage of 3.0 kV was used to collect the SEM micrographs.

Results and discussion

A one-step reactive extrusion process (Fig. 1) was used to produce the PLA-based thermoplastic materials that were biodegradable. In our approach, PHBV can go through thermal decomposition at 170 °C for obtaining oligomers consisting of vinyl groups, which can be used to graft onto PLA chains simultaneously upon initiation with the presence of PHBV. Not only this method was efficient to prepare grafted polymer blends with covalent linkages to improve their thermal and mechanical properties, but more importantly, it was a complete green and energy-saving process since it did not require the use of solvents. Different amounts of initiators compositions were used in the blending process for controlling the conversion of this grafting reaction.

As shown in Fig. 2, the thermal degradation of PHBV was known to produce oligomeric products with substituted olefins, which the chemical compositions were analyzed by ^1H NMR [42]. Figure 3 shows the chemical shift of degradation residue under air atmosphere at 170 °C for 10 min and 45 min. Substituted olefins of oligomers can be observed in both ^1H NMR spectra. The characteristic peaks associated with vinyl groups include 2.05 ppm (*i*, $\text{R}-\text{CH}=\text{CH}-$), 6.98 ppm (*m*, $\text{R}-\text{CH}=\text{CH}-$), and 5.84 ppm (*n*, $\text{R}-\text{CH}=\text{CH}-$). The increase in relative intensity of these three peaks from 10 to 45 min indicated that increasing reaction time leads to the formation of a higher amount of substituted olefin end groups. The ratio of characteristic peak *m* ($\text{R}-\text{CH}=\text{CH}-$) to *b* + *f* ($-\text{O}-\text{CH}(\text{CH}_3)-\text{CH}_2-$ or $-\text{O}-\text{CH}(\text{CH}_2\text{CH}_3)-\text{CH}_2-$)

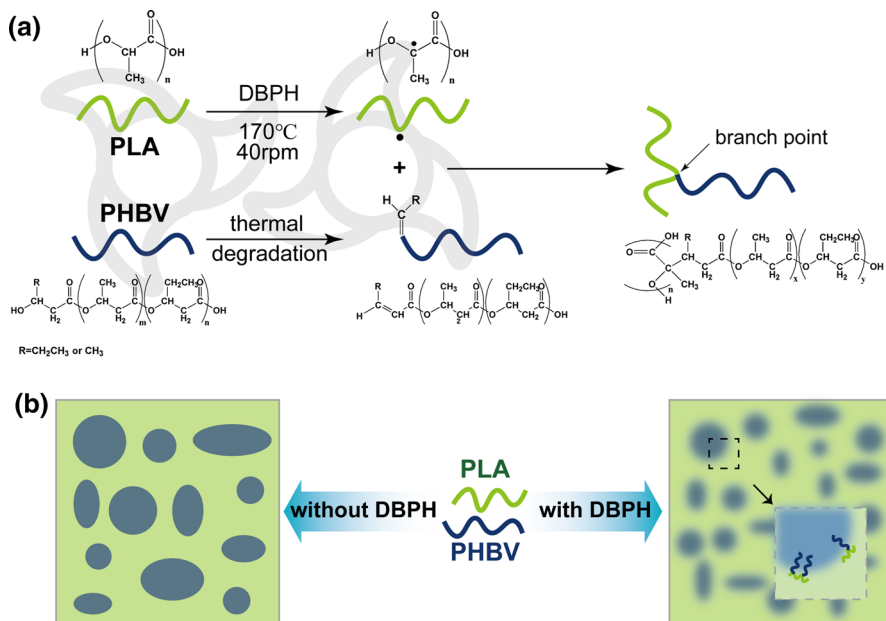


Fig. 1 **a** Schematic illustration of synthesizing PLA-g-PHBV graft copolymer during one-step reactive 12 blending; **b** schematic illustration of the in situ formation of PLA-g-PHBV copolymer at the 13 PLA/PHBV blend interface

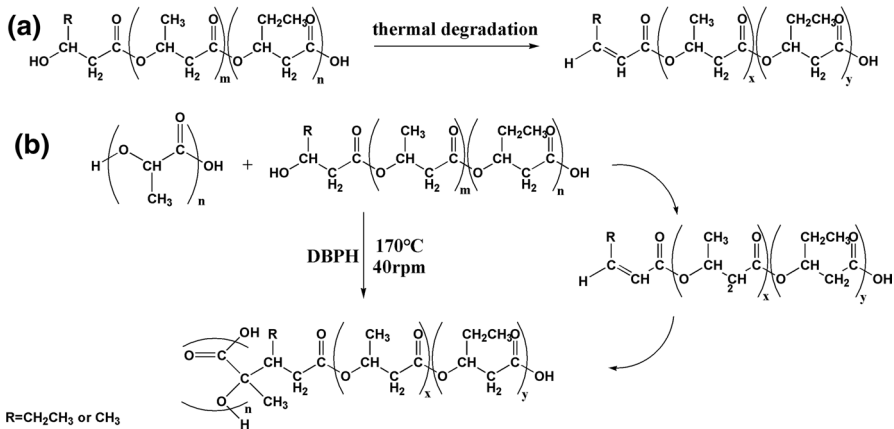
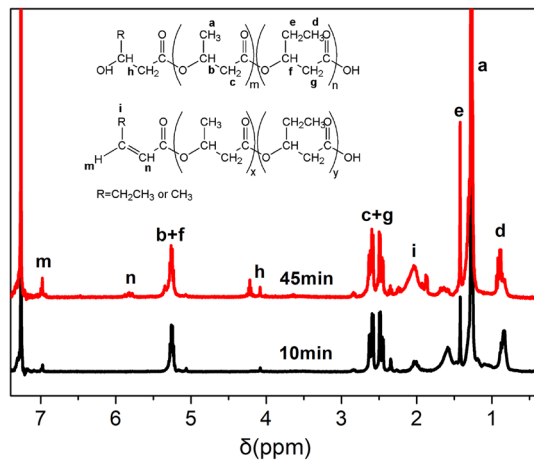


Fig. 2 Schematic presentation of **a** the thermal degradation of PHBV and **b** the grafting of the PHBV 3 to the main chain of PLA

Fig. 3 ¹H NMR spectra of the formation of thermal degraded PHBV at 170 °C for different time



increased from 0.06 (10 min) to 0.15 (45 min). Figure S1 shows the ¹H NMR spectra of neat PLA and PLA after 170 °C for 10 min. No obvious changes in chemical shift values were observed between samples before and after processing. The characteristic peak of $-\text{CH}-$ was 1.56–1.58 ppm, and that of $-\text{CH}_3$ was 5.13–5.17 ppm [46]. The proton area ratio ($-\text{CH}_3/-\text{CH}-$) was maintained at 3. The FTIR spectra of 100/0, 0/100, 80/20, and 80/20D3 are shown in Figure S2. For 100/0, a strong and sharp absorption peak was observed at 1746 cm^{-1} in the spectrum, which was due to the stretching vibration of C=O. In addition, the peaks at 1452 cm^{-1} and 1358 cm^{-1} were derived from C–H deformation vibration, and the peak at 1078 cm^{-1} was due to C–O–C stretching vibration. The peak of the C=O stretching mode of 0/100 was observed at 1719 cm^{-1} . The absorption peaks at 1274 cm^{-1} and 1043 cm^{-1} were considered to be the C–O–C stretching mode of PHBV. The absorption peak

detected at 1130 cm^{-1} was from the C–O–C stretching band [47]. For blend samples, all the characteristic groups of the raw materials were observed in the FTIR spectra.

Understanding material viscosity is important for informing their processing conditions, which can be determined by their torque and melt flow index measurements. As all raw materials were added at the same step for reactive extrusion, only one torque maximum, T_{\max} , was observed, and T_b was the balanced torque at the end of entire processing. Figure 4a shows the how torque changes as a function of time for all PLA/PHBV blends with the absence of DBPH. T_{\max} was 19.4 Nm for the sample only containing PLA, which gradually decreased with the increase in PHBV content. For the sample of 60/40, the T_{\max} was approximately at 12.2 Nm. The change of T_b was much less dependent on the inclusion of PHBV, only ranging from 1.6 to 2.5 Nm for all samples. However, when DBPH was involved in the process, T_b changed more significantly as a function of the DBPH content (Fig. 4b, c). For the 80/20 sample, when the initiator content increased from 0.1 to 0.5 wt%, T_{\max} only slight decreased from 15.4 to 13.2 Nm, and T_b increased from 2.0 Nm to 4.3 Nm. Similar trend was observed for 70/30, where T_{\max} decreased from 13.4 to 12.2 Nm, and T_b increased from 1.9 to 4.5 Nm. As the change in torque was directly related to the overall viscosity of the sample, these results demonstrate that (1) with the addition of PHBV, the intermolecular interaction between PLA chains was less pronounced, which

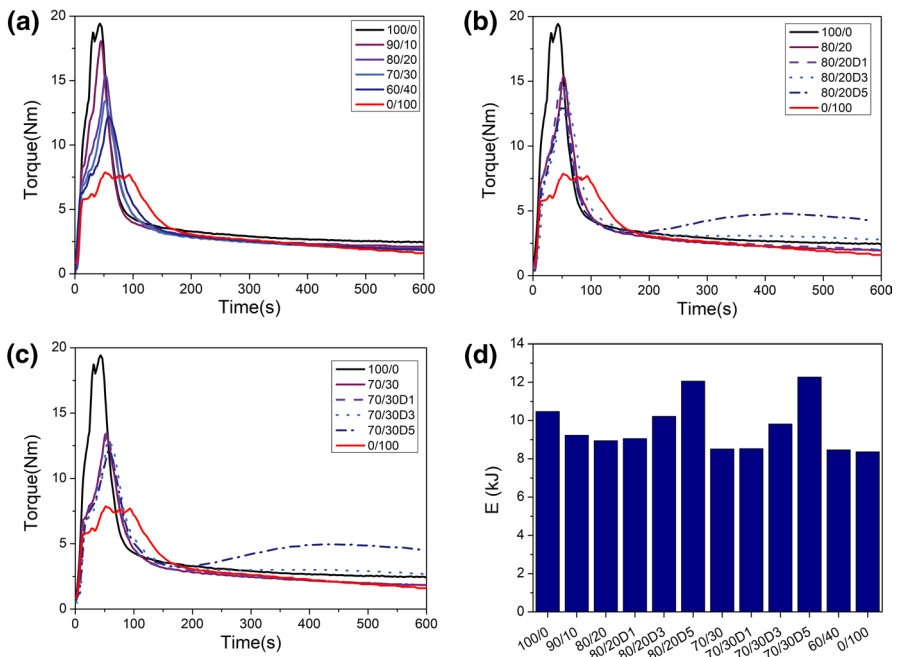


Fig. 4 **a–c** Torque change with time under different ratios of PLA/PHBV and DBPH concentrations in 9 HAAKE (time: 10 min, temperature: 170 °C, screw speed: 40 rpm/min); **d** mechanical energy required for 10 the processing of PLA/PHBV blends

contribute to the reduction in viscosity, and (2) the presence of DBPH was able to initiate the grafting reaction. At the beginning of the reaction, the initiator played a role of lubrication, so T_{max} was reduced. However, with the reaction progressing, partially degraded PHBV was grafted onto PLA, and the force between molecules changed from intermolecular force to covalent bonding, limiting the diffusion of molecular chains and leading to an increase in viscosity of the product. Furthermore, the torque used in the processing was indicative of its corresponding energy requirement. The torque curve records the mechanical energy required during processing, and it can be calculated from the area under the curve. The mechanical energy (ME) absorbed during the processing by each sample was obtained via Eq. (3):

$$ME = 2\pi N \int C(t)dt \tag{3}$$

where N is the rotational speed (rpm), $C(t)$ is the total torque used of the whole processing (Nm), and t is the processing time (min).

The mechanical energy is defined as the energy transmitted to the material during processing, corresponding to the respective processing conditions. Figure 4d shows the ME required by blends of different proportions during processing. As the initiator content increases, the energy required for processing begins to rise. The ME required to obtain 80/20D5 is 1.35 times that of 80/20, and the ME required to obtain 70/30D5 is 1.44 times that of 70/30, indicating an increased costs associated with the reactive extrusion process with the presence of initiators [48].

The changes in sample viscosity were also observed form MFI experiment, a common method to determine the flow property of polymers in the plastics processing industry [49]. As the PLA content decreased, the melt index gradually increased (Fig. 5a). When the PHBV content reached 40%, the melt index increased from 18.6 to 29.9 g/10 min. For blends containing initiator, the melt index showed a decreasing trend as the initiator content increased (Fig. 5b). Specifically, for blends containing 0.5% initiator, the melt index decreased from 22.5

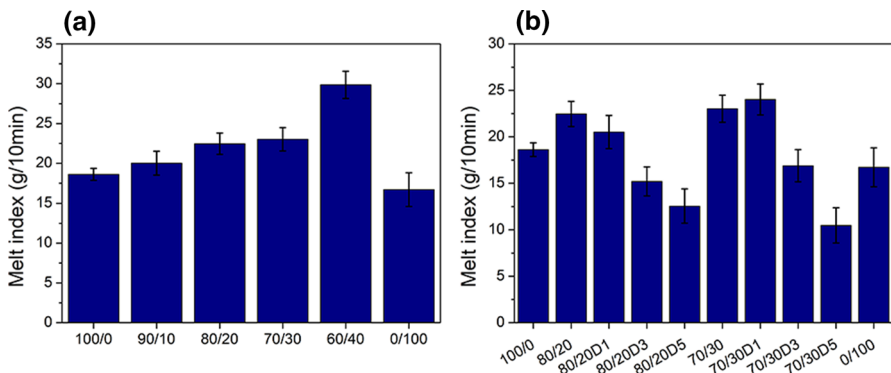


Fig. 5 Melt flow index of the PLA/PHBV blends: **a** blends in different proportions without initiator; **b** blends in different proportions with initiator

to 12.5 g/10 min (for 80/20) and from 23.0 to 10.5 g/10 min (for 70/30). This trend is consistent with the change in T_b . Similar to torque, the increase in the melt index from blending suggested that these materials could exhibit improved flow behavior for processing.

The mechanical properties of all samples, including pure PLA, pure PHBV, PHBV/PLA blends with initiator and without initiator, are shown in Fig. 6. PHBV exhibits very poor mechanical properties of both the elongation at break (3.96%) and tensile strength (33.4 MPa) due to its rigid backbone structures [50, 51]. As a comparison, PLA is typically stronger yet more brittle [37]. While pure PLA showed the elongation at break of around 5.16%, its tensile strength was 49.6 MPa. The inclusion of PHBV into PLA was able to improve the elongation at break of PLA significantly, with the compromise of tensile strength [52]. As shown in Fig. 6a, the elongation at break of the blend increased to 10.87% and 11.41%, when the mass ratio of PLA/PHBV was 80/20 and 70/30, respectively. These results were 2.11 and 2.21 times of the elongation of pure PLA and 2.74 and 2.88 times of pure PHBV. However, the tensile strength of both samples decreased to 44.78 MPa and 42.43 MPa. Additionally, at a 40 wt% of PHBV content, the elongation at break decreased significantly, exhibiting a similar value with pure PLA, which may be attributed to the occurrence of macrophase separation from the incompatibility between PLA and PHBV.

We further investigated how the presence of DBPH influences the mechanical properties of 80/20 and 70/30 (PLA/PHBV) through graft reactions. Three different initiator concentrations (0.1 wt%, 0.3 wt%, and 0.5 wt%) were employed. Figure 6b shows how the material mechanical properties changes as a function of the amount of DBPH. When the initiator was added to induce the grafting reaction during processing, the tensile strength of the blend increased significantly. For the ratio of 70/30, the addition of initiator further increased the tensile strength of the blend, while reducing the elongation at break. It was found that the tensile strength increased from 42.4 (without DBPH) to 45.8 MPa (0.5 wt% DBPH), 47.8 MPa (0.3 wt% DBPH), and 50.5 MPa (0.1 wt% DBPH), while the elongation at break reduced from 11.41 (without DBPH) to 9.00% (0.1 wt% DBPH), 8.72% (0.3 wt% DBPH) and 8.78% (0.5 wt% DBPH). Interestingly, the inclusion of initiator increased both

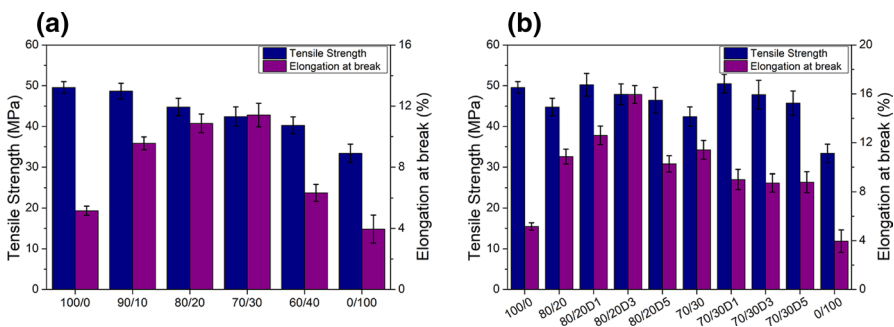
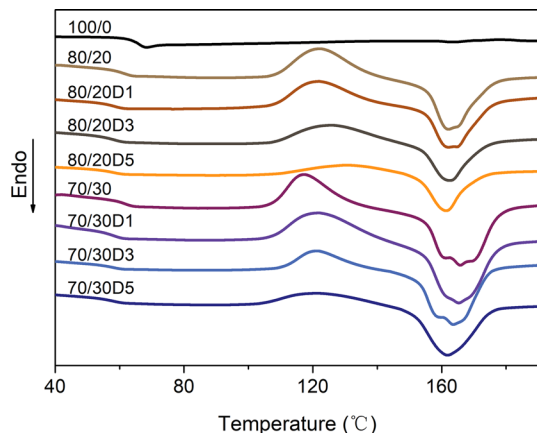


Fig. 6 Mechanical properties of the PLA/PHBV blends: **a** blends in different proportions without 12 initiator and **b** blends in different proportions with initiator

the tensile strength and the elongation at break for the composition of 80/20. The tensile strength of 80/20D1 blend already reached 50.25 MPa, exceeding that of pure PLA. The elongation at break of 80/20D3 showed the most superior performance, which was about 15.95%, 3.09 times of pure PLA and 1.47 times of the blend without the initiator. For comparison, the elongation at break of 80/20D1 and 80/20D5 was 12.60% and 10.27%, respectively, which were lower than the elongation at break of 80/20D3. However, its tensile strength was only 3.44% lower than pure PLA. Analysis of variance on the values of elongation at break and tensile strength is shown in Tables S1–S4 to prove that the increase was significant. Comparison between the tensile strength of 80/20 and 80/20D1 showed a clear difference, which is similar with 70/30 and 70/30D1, 70/30D3. Meanwhile, there was no significant difference in tensile strength between pure PLA and blends with initiator. In addition, for the polymer blends systems containing initiators, we found that only using a low amount of initiator was effective to improve the tensile strength of the blend. The elongation at break of 80/20D5 was 10.27%, and the tensile strength was 46.4 MPa, both lower than the mechanical properties of 80/20D3. When the initiator was added excessively, although the tensile strength of the product was higher than the product without initiator as well, the elongation at break became lower. The yield strength of the blend exhibited a trend similar to the tensile strength, as shown in Figure S3, with no significant difference in the modulus of elasticity of the various blends. These results suggest that the initiator may be suitable as a trace additive to improve the mechanical properties of the blend. If the degree of grafting is too high, it will adversely affect the mechanical properties.

For all thermoplastics, thermal properties are essential for determining their temperature window of processing and product use. Figure 7 shows the DSC curves of blends with different compositions, and Table S5 shows the T_g , T_m and the crystallization of the PLA/PHBV blends from DSC. The glass transition temperature (T_g) of pure PLA is around 60 °C, which is consistent with literature results, while the T_g of PHBV is approximately 0 °C. [47, 53–55]. For the PLA/PHBV blend, it can be noticed that the T_g of the PLA phase slightly decreased to 57.1–58.9 °C, suggesting

Fig. 7 DSC curves of the PLA/PHBV blends with different compositions



that two phases were partially miscible. For the grafting blends with the initiator, the PLA phase showed a lower glass transition temperature. For example, T_g of 70/30D1 was 48.6 °C, nearly 12 °C lower than that of pure PLA. We attributed this decrease in T_g to the enhanced compatibility between PLA and PHBV segments through reactive extrusion. In our system, in situ synthesized PLA-g-PHBV plays an important role for improving the miscibility, efficiently served as interfacial stabilizer. Moreover, adding PHBV promotes the PLA crystallization as evidenced by the peaks in the DSC curves of all samples, which can be possibly explained by that PHBV acts as a nucleating agent. With increase in the initiator content, the crystallization temperature of the blend increased, and the crystallization enthalpy decreased. The peroxide initiated the grafting reaction, which also formed branch point, effectively serving as nucleating agents in the crystallization process. Studies suggested that branch point of long-chain-branched PLA can act as a nucleation point to lead to a faster crystallization rate [56]. Higher amount of initiator loading would result in the formation of more branching points. The presence of branched molecules can hinder the diffusion of PLA chains, and thus, a higher temperature was required for the crystallization of PLA phase. After blending with PHBV, the DSC curve showed multiple melting peaks due to the following reasons: (1) melting, recrystallization, and remelting during heating; (2) isodimorphism or polymorphism, which is the presence of multiple crystal forms, and (3) different lamellar thickness, distribution, and morphology, and species with different molecular weight. The co-crystallization behavior can also promote heterogeneous nucleation, thus inducing a faster crystallization rate and improved crystal perfection during the melting process [57]. However, with the increase in the initiator content, the multiple peaks gradually become a single peak, and the melting temperature decreased.

Thermal stability of neat, blended, and grafted PLA/PHBV was investigated by TGA at the heating rate of 10 °C/min under nitrogen atmosphere, as illustrated in Fig. 8a. All thermal degradation parameters of the PLA/PHBV blends are shown in Table S6. The thermal decomposition temperature of PLA and PHBV was 366.6 °C and 295.3 °C, respectively, indicating PLA was more thermally stable than PHBV [57]. The blends exhibited higher thermal stability than PHBV, but lower than PLA, with all samples showing two peaks from the DTG curves (Fig. 8b). The two-step

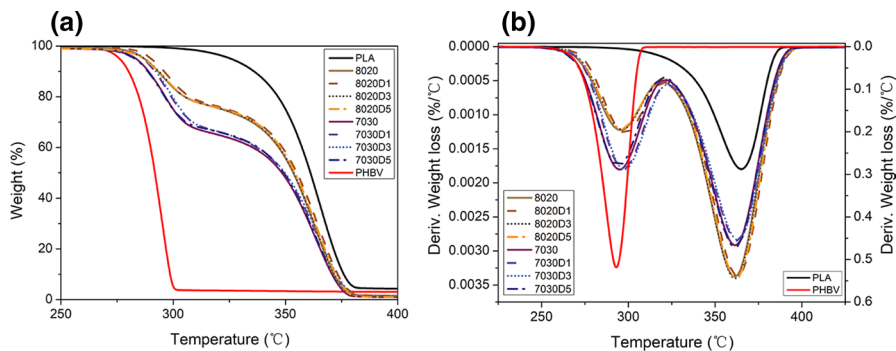


Fig. 8 Thermogravimetric curves for the PLA/PHBV blends: **a** TG; **b** DTG

weight loss was corresponded to PHBV (at 294.33–300.17 °C), and PLA phase (at 362.33–365.5 °C), similar to the observation from Zembouai et al. [47]. Furthermore, the degree of weight loss at each step corresponds well with the blend composition, which is consistent for all samples. It is noted that the presence of initiator for triggering grafting reactions does not have a pronounced impact on the thermal decomposition temperatures of blend samples.

X-ray diffraction also confirmed the crystalline properties of the blend, as shown in Fig. 9. The addition of PHBV improves the degree of crystallization of PLA (shown in Table S6). After PHBV was introduced, diffraction peaks were observed in the blends, which were different from the typical amorphous peaks of pure PLA. The lattice planes (010), (200)/(110), (203), and (015) of PLA α -crystal correspond to the characteristic peaks $2\theta=13.7^\circ$, 16.6° , 20.0° and 22.6° , respectively [58]. With the increase in the peroxide initiator content in the blend increased, diffraction peaks become more pronounced, indicating that the crystallinity of the blend has increased, which was consistent with the DSC results.

Figure 10 shows the weight loss for the PLA/PHBV blends in phosphate-buffered saline at 80 °C. The temperature used for the experiment was higher than the glass transition temperature of all blends, so the hydrolysis reaction can be accelerated, and the hydrolysis of blends of different proportions has been observed. After 2 weeks of hydrolysis, PLA had the highest degree of hydrolysis, reaching 61.67%. The 70/30 with higher PHBV content had the least degree of hydrolysis, but it also reached 44.19%. As the content of DBPH in the blend increases, the hydrolysis reaction became faster. Compared with 80/20, 80/20D5 has a 6.35% increase in the weight loss. Meanwhile, the weight loss of 70/30D5 was 4.39% higher than that of 70/30. After 1 day of hydrolysis, all the samples were broken, showing a rapid decline in mechanical properties. These results confirmed that the products after blending modification retain the hydrolysis characteristics of the two raw materials.

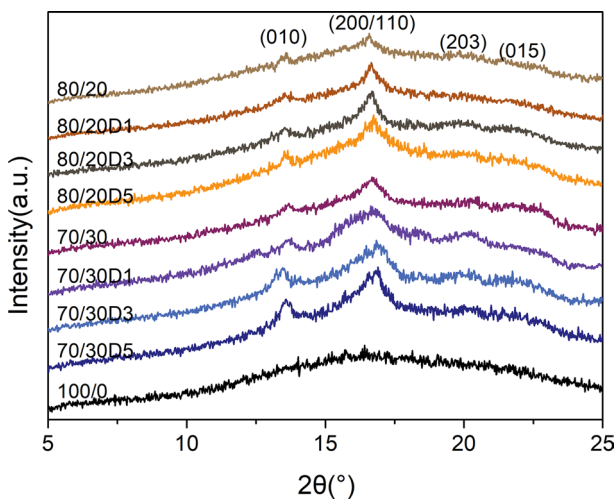


Fig. 9 XRD patterns of the PLA/PHBV blends with different compositions

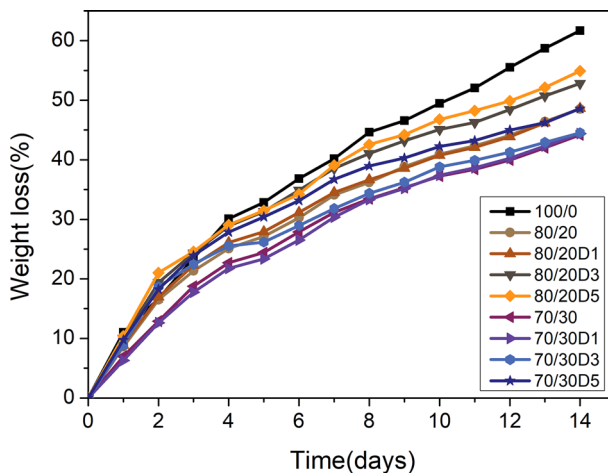


Fig. 10 Weight loss as a function of time for the PLA/PHBV blends in phosphate-buffered saline at 80 °C

Finally, SEM was used to determine the morphology of blend samples. Morphology of polymer blends can largely impact their physical properties and rheological behaviors [28]. Figure 11 shows the SEM micrographs of the fractured surface of PLA/PHBV blends with or without DBPH, which were obtained from cryo-fracturing. For the blends without initiators, PHBV particles and dark holes were observed on the surface of the blends with PLA as matrix (Fig. 11a, e). For blends with higher PHBV content, the domain sizes became clearly larger with a broader distribution. The surface of these particles seemed to have web-like entanglements slightly penetrating into the surrounding areas for PLA. The connection of PHBV with PLA was not tight, evidenced by the visible cavity around the spherical domains. This was an indication that PHBV and PLA form a two-phase system. With the addition of the initiator, the size of PHBV domains gradually decreased, and the interface between the PLA and PHBV phases gradually became more blurred. The bridge between PHBV and PLA became more and wider, which illustrated the PHBV phase was wrapped by PLA, or incorporated into PLA (Fig. 11b–d, f–h). Furthermore, the morphology of the blend changed from a typical sea-island structure to a layered structure, suggesting that increasing the initiator content would result in further improved compatibility between the two phases.

The PLA/PHBV blends exhibited neck formation and growth during tensile test by a considerable stress-whitening volume [59]. The stress whitening is a consequence of numerous cavities and/or crazes formed during deformation in general. In rubber-toughened polymers, two types of cavitation processes can be formed, which are internal rubber cavitation and interfacial debonding. Both cavitation processes are beneficial for improving the toughness of blends. Moderate interfacial adhesion between PLA and PHBV phases and suitable PHBV particle size enables both types of cavitation formed during tensile tests. The mode of cavitation process depends on a competition between the energy

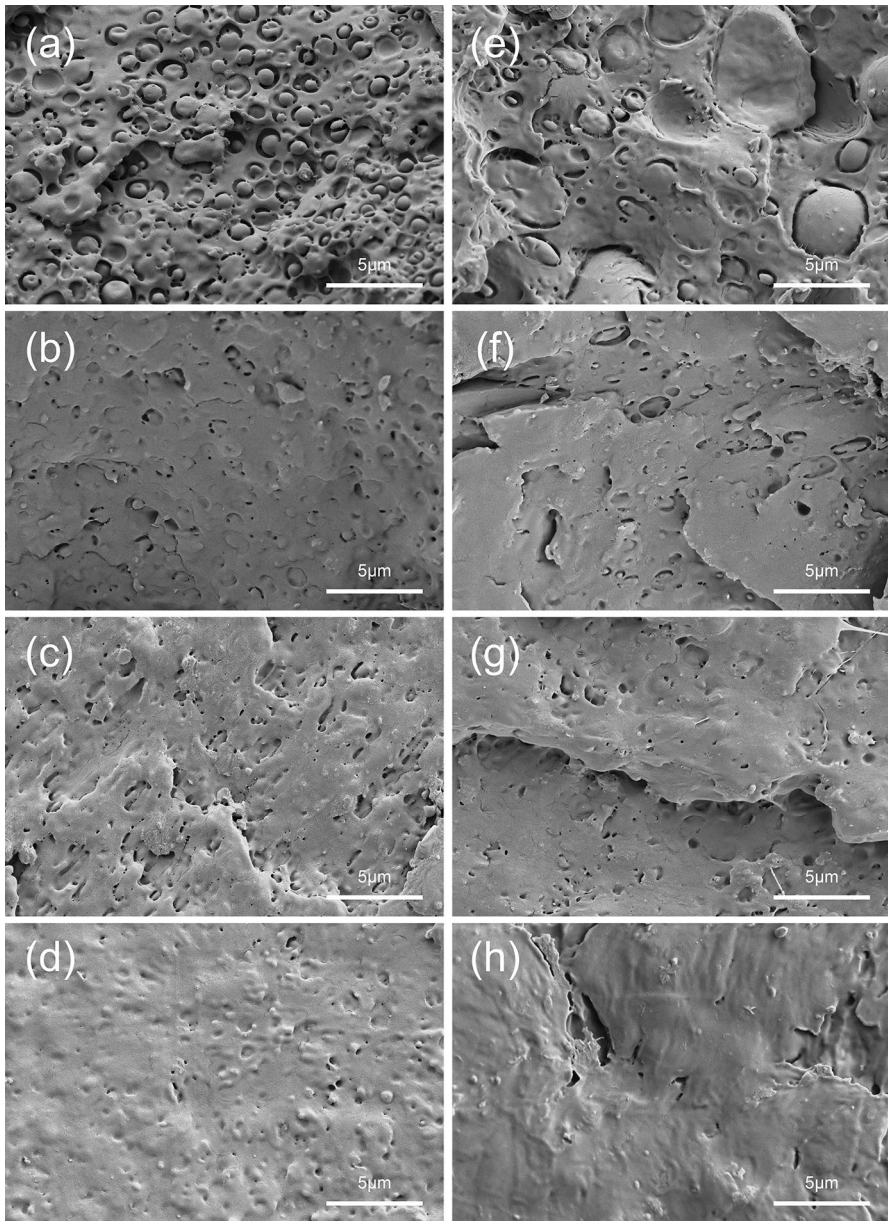


Fig. 11 SEM micrographs of fractured surface of PLA/PHBV blends with or without DBPH: **a** 80/20; **b** 80/20D1; **c** 80/20D3; **d** 80/20D5; **e** 70/30; **f** 70/30D1; **g** 70/30D3; **h** 70/30D5.

gained by relieving the stress via cavitation and the energy needed to create a new surface inside of the rubber. With the increase in the initiator content, the particle size of the PHBV phase was too small, and the connection with the PLA phase was too tight, which was not conducive to toughening. It causes the elongation at

break to decrease as the initiator content increases. In terms of the PLA/PHBV blend, phase separation can occur due to the chemical incompatibility between PLA and PHBV, resulting in low mechanical strength. With the addition of the initiator, the compatibility of the two phases was improved, which was conducive to the improvement of the tensile strength. However, the increased compatibility changed the size of the PHBV phase and the connection between the two phases. Therefore, as the degree of grafting increased, the tensile strength decreased. In addition, the crystallinity of the blend also affected the tensile strength. The increase in crystallinity in a small range was conducive to the improvement of tensile strength. Too high also reduced the tensile strength. The compatibility of the two phases and the crystallinity of the blend affected the tensile strength together [60].

Conclusion

In conclusion, the properties and structure of the PLA/PHBV blends have been systematically studied with the focus on understanding the impact of the peroxide initiator (DBPH) addition. The blends were obtained through a one-step reactive extrusion process. The torque curve shows the change of the melt state with the progress during the one-step process, and the melt index drops from 23.0 for PLA to 10.5 g/10 min for 70/30D5. The grafted PLA/PHBV blends initiated by DBPH could significantly increase the elongation at break while retaining excellent tensile strength. The elongation at break of 80/20D3 is about 15.95%, while the tensile strength is very similar to the pure PLA. Therefore, 80/20D3 is considered to be the optimized ratio among all components. Differential scanning calorimetry and thermogravimetric analysis illustrate that the melting point of the blends with the initiators decreases, the thermal decomposition temperature increases, suggesting the possible broader processing conditions. All blends exhibited hydrolyzability at a temperature slightly higher than the glass transition temperature of PLA components. SEM micrographs of the fractured surface of PLA/PHBV blends show the change of blend microstructure from sea-island to layered, confirming the improved compatibility from our grafting reactions. Overall, we believe that blending of PLA and PHBV with grafting reaction is an effective and feasible method to obtain green degradable bio-based thermoplastics, which also provides the opportunity for controlling the material properties by simply adjusting the ratio between components.

Supplementary Information The online version contains supplementary material available at <https://doi.org/10.1007/s00289-021-03958-6>.

Acknowledgements This work was financially supported by the Shanghai 2020 “Science and Technology Innovation Action Plan” Social Development Science and Technology Research Project (20dz1203600), the Fundamental Research Funds for the Central Universities, and the Open Funds for Characterization of Tongji University. Z.Q. acknowledges generous financial support from the University of Southern Mississippi.

References

1. Guzdemir OO, Bermudez V, Kanhere S, Ogale AA (2020) Melt-spun poly(lactic acid) fibers modified with soy fillers: toward environment-friendly disposable nonwovens. *Polym Eng Sci* 60:1158–1168. <https://doi.org/10.1002/pen.25369>
2. Pan G, Xu H, Ma B, Wizi J, Yang Y (2018) Polylactide fibers with enhanced hydrolytic and thermal stability via complete stereo-complexation of poly(L-lactide) with high molecular weight of 600000 and lower-molecular-weight poly(D-lactide). *J Mater Sci* 53:5490–5500. <https://doi.org/10.1007/s10853-017-1944-2>
3. Jayanth D, Kumar PS, Nayak GC, Kumar JS, Pal SK, Rajasekar R (2018) A review on biodegradable polymeric materials striving towards the attainment of green environment. *J Polym Environ* 26:838–865. <https://doi.org/10.1007/s10924-017-0985-6>
4. Muthuraj R, Misra M, Mohanty AK (2018) Biodegradable compatibilized polymer blends for packaging applications: a literature review. *J Appl Polym Sci* 135:45726. <https://doi.org/10.1002/app.45726>
5. Thulasingh A, Kumar K, Yamunadevi B, Poojitha N, SuhailMadharHanif S, Kannaiyan S (2021) Biodegradable packaging materials. *Polym Bull.* <https://doi.org/10.1007/s00289-021-03767-x>
6. Scaffaro R, Maio A, Sutura F, Gulino EF, Morreale M (2019) Degradation and recycling of films based on biodegradable polymers: a short review. *Polymers* 11:651. <https://doi.org/10.3390/polym11040651>
7. Larranaga A, Lizundia E (2019) A review on the thermomechanical properties and biodegradation behaviour of polyesters. *Eur Polymer J* 121:109296. <https://doi.org/10.1016/j.eurpolymj.2019.109296>
8. Nofar M, Sacligil D, Carreau PJ, Kamal MR, Heuzey MC (2018) Poly (lactic acid) blends: processing, properties and applications. *Int J Biol Macromol* 125:307–360. <https://doi.org/10.1016/j.ijbiomac.2018.12.002>
9. Purnama P, Lim SH, Kim JSH (2012) Stereocomplex-nanocomposite formation of polylactide/fluorinated-clay with superior thermal property using supercritical fluid. *Macromol Res* 20:545–548. <https://doi.org/10.1007/s13233-012-0092-4>
10. Farah S, Anderson DG, Langer R (2016) Physical and mechanical properties of PLA, and their functions in widespread applications—a comprehensive review. *Adv Drug Deliv Rev* 107:367–392. <https://doi.org/10.1016/j.addr.2016.06.012>
11. Masutani K, Kobayashi K, Kimura Y, Lee CW (2018) Properties of stereo multi-block polylactides obtained by chain-extension of stereo tri-block polylactides consisting of poly(L-lactide) and poly(D-lactide). *J Polym Res* 25:74. <https://doi.org/10.1007/s10965-018-1444-3>
12. Murariu M, Dubois P (2016) PLA composites: from production to properties. *Adv Drug Deliv Rev* 107:17–46. <https://doi.org/10.1016/j.addr.2016.04.003>
13. Chalermpanaphan V, Chochottiros C (2021) Synthesis of unsaturated aliphatic polyester-based copolymer: effect on the ductility of PLA blend and crosslink. *Polym Bull.* <https://doi.org/10.1007/s00289-021-03596-y>
14. Zhou Y, Wang J, Cai SY, Wang ZG, Zhang NW, Ren J (2018) Effect of POE-g-GMA on mechanical, rheological and thermal properties of poly(lactic acid)/poly(propylene carbonate) blends. *Polym Bull* 75:5437–5454. <https://doi.org/10.1007/s00289-018-2339-5>
15. Tebaldi ML, Chaves Maia AL, Poletto F, de Andrade FV, Ferreira Soares DC (2019) Poly(-3-hydroxybutyrate-co-3-hydroxyvalerate) (PHBV): current advances in synthesis methodologies, antitumor applications and biocompatibility. *J Drug Delivery Sci Technol* 51:115–126. <https://doi.org/10.1016/j.jddst.2019.02.007>
16. Goonoo N, Bhaw-Luximon A, Passanha P, Esteves SR, Jhurry D (2017) Third generation poly(hydroxyacid) composite scaffolds for tissue engineering. *J Biomed Mater Res Part B-Appl Biomater* 105:1667–1684. <https://doi.org/10.1002/jbm.b.33674>
17. Rivera-Briso AL, Serrano-Aroca A (2018) Poly(3-hydroxybutyrate-co-3-hydroxyvalerate): enhancement strategies for advanced applications. *Polymers* 10:732. <https://doi.org/10.3390/polym10070732>
18. Ling C, Qiao GQ, Shuai BW, Song KN, Yao WX, Jiang XR, Chen GQ (2019) Engineering self-floculating *Halomonas campaniensis* for wastewaterless open and continuous fermentation. *Biotechnol Bioeng* 116:805–815. <https://doi.org/10.1002/bit.26897>

19. Mooninta S, Poompradub S, Prasassarakich P (2020) Packaging film of PP/LDPE/PLA/Clay composite: physical, barrier and degradable properties. *J Polym Environ* 28:3116–3128. <https://doi.org/10.1007/s10924-020-01840-6>
20. You X, Snowdon MR, Misra M, Mohanty AK (2018) Biobased poly(ethylene terephthalate)/poly(lactic acid) blends tailored with epoxide compatibilizers. *ACS Omega* 3:11759–11769. <https://doi.org/10.1021/acsomega.8b01353>
21. Srisuwan S, Ruksakulpiwat Y, Chumsamrong P (2020) Effect of triblock copolymers based on liquid natural rubber and low molecular weight poly(lactic acid) on physical properties of poly(lactic acid)/natural rubber blend. *Polym Bull* 78:1253–1273. <https://doi.org/10.1007/s00289-020-03158-8>
22. Lei W, Yang X, Qiao H, Dean S, Wang R, Zhang L (2018) Renewable resource-based elastomer nanocomposite derived from myrcene, ethanol, itaconic acid and nanosilica: design, preparation and properties. *Eur Polym J* 106:1–8. <https://doi.org/10.1016/j.eurpolymj.2018.04.006>
23. Dhaliwal GS, Anandan S, Chandrashekhara K, Lees J, Nam P (2018) Development and characterization of polyurethane foams with substitution of polyether polyol with soy-based polyol. *Eur Polymer J* 107:105–117. <https://doi.org/10.1016/j.eurpolymj.2018.08.001>
24. Sahu P, Bhowmick AK, Kali G (2020) Terpene based elastomers: synthesis, properties, and applications. *Processes* 8:553. <https://doi.org/10.3390/pr8050553>
25. Alias NF, Ismail H (2019) An overview of toughening polylactic acid by an elastomer. *Polym-Plast Technol Mater* 58:1399–1422. <https://doi.org/10.1080/25740881.2018.1563118>
26. Zhang H, Deng B, Liu Q, Cong W (2015) Blends of polylactide and poly(3-hydroxybutyrate-co-3-hydroxyvalerate) with low content of hydroxyvalerate unit: morphology, structure, and property. *J Appl Polym Sci* 132:42689. <https://doi.org/10.1002/app.42689>
27. Jost V, Miesbauer O (2017) Effect of different biopolymers and polymers on the mechanical and permeation properties of extruded PHBV cast films. *J Appl Polym Sci* 135:46153. <https://doi.org/10.1002/app.46153>
28. Zhang K, Mohanty AK, Misra M (2012) Fully biodegradable and biorenewable ternary blends from polylactide, poly(3-hydroxybutyrate-co-hydroxyvalerate) and Poly(butylene succinate) with balanced properties. *ACS Appl Mater Interfaces* 4:3091–3101. <https://doi.org/10.1021/am3004522>
29. Li LZ, Huang W, Wang BJ, Wei WF, Gu Q, Chen P (2015) Properties and structure of polylactide/poly(3-hydroxybutyrate-co-3-hydroxyvalerate) (PLA/PHBV) blend fibers. *Polymer* 68:183–194. <https://doi.org/10.1016/j.polymer.2015.05.024>
30. Formela K, Zedler L, Hejna A, Tercjak A (2018) Reactive extrusion of bio-based polymer blends and composites—current trends and future developments. *Express Polym Lett* 12:24–57. <https://doi.org/10.3144/expresspolymlett.2018.4>
31. Yves Y, Benjamin G, Nicolas LM, Marion J, Frédéric L, Jean M, Thomas XM (2018) Peptide couplings by reactive extrusion: solid-tolerant and free from carcinogenic, mutagenic and reprotoxic chemicals. *Acs Sustain Chem Eng* 6:16001–16004. <https://doi.org/10.1021/acssuschemeng.8b04509>
32. Zhao D, Yan D, Zhang N, Yang G (2019) Preparation of super-toughened PA6 with submicronized ABS by in situ reactive extrusion method. *Mater Lett* 251:18–22. <https://doi.org/10.1016/j.matlet.2019.05.029>
33. Rigoussen A, Verge P, Raquez JM, Habibi Y, Dubois P (2017) In-depth investigation on the effect and role of cardanol in the compatibilization of PLA/ABS immiscible blends by reactive extrusion. *Eur Polymer J* 93:272–283. <https://doi.org/10.1016/j.eurpolymj.2017.06.004>
34. Wang Y, Mei Y, Wang Q, Wei W, Huang F, Li Y, Li J, Zhou Z (2019) Improved fracture toughness and ductility of PLA composites by incorporating a small amount of surface-modified helical carbon nanotubes. *Compos Part B-Eng* 162:54–61. <https://doi.org/10.1016/j.compositesb.2018.10.060>
35. Wang M, Wu Y, Li YD, Zeng JB (2017) Progress in toughening poly(lactic acid) with renewable polymers. *Polym Rev* 57:557–593. <https://doi.org/10.1080/15583724.2017.1287726>
36. Zhang NW, Zeng C, Wang L, Ren J (2012) Preparation and properties of biodegradable poly(lactic acid)/poly(butylene adipate-co-terephthalate) blend with epoxy-functional styrene acrylic copolymer as reactive agent. *J Polym Environ* 21:286–292. <https://doi.org/10.1007/s10924-012-0448-z>
37. Mo XZ, Wei FX, Tan DF, Pang JY, Lan CB (2020) The compatibilization of PLA-g-TPU graft copolymer on polylactide/thermoplastic polyurethane blends. *J Polym Res* 27:33. <https://doi.org/10.1007/s10965-019-1999-7>
38. Wang FY, Dai L, Ge TT, Yue CB, Song YM (2020) alpha-methylstyrene-assisted maleic anhydride grafted poly(lactic acid) as an effective compatibilizer affecting properties of microcrystalline cellulose/poly(lactic acid) composites. *Express Polym Lett* 14:530–541. <https://doi.org/10.3144/expresspolymlett.2020.43>

39. Marsilla KIK, Verbeek CJR (2017) Crystallization of itaconic anhydride grafted poly(lactic acid) during annealing. *J Appl Polym Sci* 134:44614. <https://doi.org/10.1002/app.44614>
40. Abdelwahab MA, Jacob S, Misra M, Mohanty AK (2021) Super-tough sustainable biobased composites from polylactide bioplastic and lignin for bio-elastomer application. *Polymer* 212:123153. <https://doi.org/10.1016/j.polymer.2020.123153>
41. Bäckström E, Odelius K, Hakkarainen M (2019) Designed from recycled: turning polyethylene waste to covalently attached polylactide plasticizers. *ACS Sustain Chem Eng* 7:11004–11013. <https://doi.org/10.1021/acssuschemeng.9b02092>
42. Xiang H, Wen X, Miu X, Li Y, Zhou Z, Zhu M (2016) Thermal depolymerization mechanisms of poly(3-hydroxybutyrate-co-3-hydroxyvalerate). *Prog Nat Sci Mater Int* 26:58–64. <https://doi.org/10.1016/j.pnsc.2016.01.007>
43. Nguyen S, Yu GE, Marchessault RH (2002) Thermal degradation of poly(3-hydroxyalkanoates): preparation of well-defined oligomers. *Biomacromol* 3:219–224. <https://doi.org/10.1021/bm0156274>
44. Hablot E, Bordes P, Pollet E, Avérous L (2008) Thermal and thermo-mechanical degradation of poly(3-hydroxybutyrate)-based multiphase systems. *Polym Degrad Stab* 93:413–421. <https://doi.org/10.1016/j.polymdegradstab.2007.11.018>
45. Du J, Wang Y, Xie X, Xu M, Song Y (2017) Styrene-assisted maleic anhydride grafted poly(lactic acid) as an effective compatibilizer for wood flour/poly(lactic acid) bio-composites. *Polymers* 9:623. <https://doi.org/10.3390/polym9110623>
46. Zhou KY, Li JB, Wang HX, Ren J (2017) Effect of Star-shaped chain architectures on the polylactide stereocomplex crystallization behaviors. *Chin J Polym Sci* 35:974–991. <https://doi.org/10.1007/s10118-017-1935-4>
47. Zembouai I, Kaci M, Bruzaud S, Benhamida A, Grohens Y (2013) A study of morphological, thermal, rheological and barrier properties of Poly(3-hydroxybutyrate-co-3-hydroxyvalerate)/polylactide blends prepared by melt mixing. *Polym Testing* 32:842–851. <https://doi.org/10.1016/j.polymertesting.2013.04.004>
48. Martins AB, Santana R (2019) Structure-properties correlation in PP/thermoplastic starch blends containing sustainable compatibilizer agent. *Mater Res Express* 6:095336. <https://doi.org/10.1088/2053-1591/ab0f73>
49. Teng CC, Ma CCM, Huang YW, Yuen SM, Weng CC, Chen CH, Su SF (2008) Effect of MWCNT content on rheological and dynamic mechanical properties of multiwalled carbon nanotube/polypropylene composites. *Compos A Appl Sci Manuf* 39:1869–1875. <https://doi.org/10.1016/j.compositesa.2008.09.004>
50. Du J, Guomin Z, Mingzhu P, Leilei Z, Dagang L, Rui Z (2017) Crystallization and mechanical properties of reinforced PHBV composites using melt compounding: effect of CNCs and CNFs. *Carbohydr Polym* 168:255–262. <https://doi.org/10.1016/j.carbpol.2017.03.076>
51. Zhao X, Cornish K, Vodovotz Y (2019) synergistic mechanisms underlie the peroxide and coagent improvement of natural-rubber-toughened poly(3-hydroxybutyrate-co-3-hydroxyvalerate) mechanical performance. *Polymers* 11:565. <https://doi.org/10.3390/polym11030565>
52. Liu G, Zhang X, Wang D (2015) Tailoring crystallization: towards high-performance poly(lactic acid). *Adv Mater* 26:6905–6911. <https://doi.org/10.1002/adma.201305413>
53. Greco A, Ferrari F, Maffezzoli A (2018) Thermal analysis of poly(lactic acid) plasticized by cardanol derivatives. *J Therm Anal Calorim* 134:559–565. <https://doi.org/10.1007/s10973-018-7059-4>
54. Leones A, Sonseca A, Lopez D, Fiori S, Peponi L (2019) Shape memory effect on electrospun PLA-based fibers tailoring their thermal response. *Eur Polymer J* 117:217–226. <https://doi.org/10.1016/j.eurpolymj.2019.05.014>
55. Jost V, Kopitzky R (2015) Blending of Polyhydroxybutyrate-co-valerate with polylactic acid for packaging applications—reflections on miscibility and effects on the mechanical and barrier properties. *Chem Biochem Eng Q* 29:221–246
56. Yang X, Clénet J, Xu H, Odelius K, Hakkarainen M (2015) Two step extrusion process: from thermal recycling of phb to plasticized PLA by reactive extrusion grafting of PHB degradation products onto PLA chains. *Macromolecules* 48:2509–2518. <https://doi.org/10.1021/acs.macromol.5b00235>
57. Zhao H, Cui Z, Sun X, Turg LS, Peng X (2013) Morphology and properties of injection molded solid and microcellular polylactic acid/polyhydroxybutyrate-valerate (PLA/PHBV) blends. *Ind Eng Chem Res* 52:2569–2581. <https://doi.org/10.1021/ie301573y>

58. Salahuddin N, Gaber M, Elneanaey S, Snowdon MR, Abdelwahab MA (2021) Co-delivery of norfloxacin and tenoxicam in Ag–TiO₂/poly(lactic acid) nanohybrid. *Int J Biol Macromol* 180:771–781. <https://doi.org/10.1016/j.ijbiomac.2021.03.033>
59. Ma P, Spoelstra AB, Schmit P, Lemstra PJ (2013) Toughening of poly (lactic acid) by poly (β -hydroxybutyrate-co- β -hydroxyvalerate) with high β -hydroxyvalerate content. *Eur Polymer J* 49:1523–1531. <https://doi.org/10.1016/j.eurpolymj.2013.01.016>
60. Ma P, Cai X, Zhang Y, Wang S, Dong W, Chen M, Lemstra PJ (2014) *In-situ* compatibilization of poly(lactic acid) and poly(butylene adipate-co-terephthalate) blends by using dicumyl peroxide as a free-radical initiator. *Polym Degrad Stab* 102:145–151. <https://doi.org/10.1016/j.polymdegradstab.2014.01.025>

Publisher's Note Springer Nature remains neutral with regard to jurisdictional claims in published maps and institutional affiliations.